Transactions of The Indian Institute of Metals
Vol. 62, Issues 4-5, August-October 2009, pp. 433-436

In-situ observation of unsteady peritectic growth modes

Andreas Ludwig, Johann Mogeritsch and Monika Grasser

Department of Metallurgy, University of Leoben, Austria

E-mail : ludwig@unileoben.ac.at

Received 04 September 2009
Revised 20 October 2009
Accepted 21 October 2009
Online at www.springerlink.com

Keywords:
peritectic solidification; solid/liquid interface morphology; organic model alloy; bridgman furnace

Abstract

A transparent non-facetted/non-facetted peritectic system was used for in-situ studies of peritectic growth morphologies above and below the limit of constitutional undercooling. For a hypo-peritectic alloy with near peritectic composition an oscillatory growth mode was found for velocities in the cellular/dendritic regime. It is demonstrated that the co-existence of two distinct cellular/dendritic solid/liquid interfaces which try to reach stable growth conditions causes this oscillations. Additionally, it is shown that on reducing the withdrawal speed the two distinct interfaces arrange into an isothermal coupled peritectic growth mode.

Introduction

Many transparent organic substances and their alloys have been investigated to find model systems that allow in-situ and real time observations of metal-like solidification phenomena such as dendritic, cellular or eutectic growth morphologies [1-6]. However, very few transparent organic systems have been reported to show a non-facetted/non-facetted (nf/nf) peritectic reaction in a temperature range suitable for direct observation in a Bridgman furnace set-up. Barrio et al. [1] reported a peritectic phase diagram for the organic model alloy NPG (Neopentylglycol)-TRIS (Tris(hydroxylmenthyl)aminomethane) which was recently confirmed by [7]. Both substances show an orientationally disordered crystalline phase at high temperature, generally called the "plastic" phase. Fig. 1 shows the phase diagram area important for peritectic solidification.

A peritectic reaction is known as a transformation where one solid phase reacts with a liquid phase on cooling to produce a second solid phase β. At the peritectic temperature, T_p, the three phases are in equilibrium with each other. The corresponding concentration of the α phase is c_α, of the β phase c_β (the so-called peritectic concentration), and of the liquid c_L. From a thermodynamic point of view, an alloy with a concentration c_0 with $c_\alpha < c_0 < c_L$ should start to solidify with the so-called properitectic α phase and transforms to the peritectic β phase when passing T_p. In practice, it is found that, for alloys with $c_\alpha < c_0 < c_\beta$, two metastable two-phase microstructures occur: (i) oscillations of the concentration in liquid adjacent to the interface forming an alternating sequence of α and β bands parallel to the solidification front (banded microstructures) [8,9] and (ii) simultaneous growth of α and β phases in the form of fibres or lamellae, similar to an regular eutectic growth front [10-15].

In order to indicate which growth mode occurs for given concentration c_0, temperature gradient G, and growth velocity, V, the corresponding morphology is often mapped as a function of alloy composition and G/V ratio [10]. In [16] it is reported, that at a high G/V ratio, α/β bands occur preferentially, whereas, at an intermediate G/V ratio, mixed bands (cellular α / plane front β) or simultaneous (coupled) growth (α+β) appear. The simultaneous growth has been observed in three systems: Ni-Al, Fe-Ni and Sn-Cu. In the peritectic Ni-Al alloys [17] and contrary to kinetic considerations the growth temperature has been shown to be below T_p. This means that the undercooling cannot be dominated by diffusional requirements, but perhaps by capillary effects. Lee and Verhoeven [17] suggested that the curvature of the peritectic phase may increase close to its centreline, similar to an interface shape for eutectics suggested by Hunt and Chilton [18], but they could not demonstrate this experimentally. The G/V-c_0 microstructure map in the hypo-peritectic range was investigated for the Fe-Ni system by [11-13] and for the Cu-Sn system by [14,15]. Numerous microstructures were found: isothermal coupled growth, with both lamellar and fibrous morphologies, island banding, cellular coupled growth and dendritic growth. It was also shown that isothermal coupled peritectic growth is promoted by a chemical composition close to the peritectic composition, and/or a high thermal gradient.

The application of synchrotron X-ray imaging has recently been demonstrated to be a suitable tool for in-situ observations of directional solidification of Al- and Sn-based alloys [19,20]. However, to the authors' knowledge no study on peritectic solidification has been done with this new technique so far.

In the present paper we report about in-situ observations of oscillatory and isothermal coupled growth morphologies for a near peritectic NPG-TRIS alloy been directional solidified in a micro-Bridgman furnace with a fixed temperature gradient.

Materials and methods

The organic substances NPG and TRIS were purchased from Aldrich [21] with an indicated purity of 99 % and 99.9+ %, respectively. Both compounds are reported to be highly hydroscopic [22]. In accordance with the material

preparation published in [1], the water content of NPG was reduced keeping the material in a dry atmosphere at 310 K for 24 hours. TRIS was used as delivered. Different types of sample geometries and sealing substances/procedures were tested. Due to the relatively high hot zone temperature necessary for peritectic solidification experiments many tested sealing materials such as UV hardening and silica-based glues started leaking after some hours. The best results were obtained using large rectangle tubes (2000 μm x 100 μm inner diameter and 100 μm wall thickness [23]) with glued ends. The alloy and sample preparation was performed within an Argon-filled glove box. The humidity within the glove box was reduced to below 10^4 ppm and the oxygen content below 2×10^3 ppm, estimated with a hygrometer and an air oxygen measuring device. For the preparation of the different alloy compositions the pure substances were weighed and joined in small glass containers which were closed with plastic caps afterwards. Next, the glass container was heated on a hot plate until the organic powder melted, then it was shaken to improve the mixing and then slowly solidified (~ 1 hour). This procedure lead to a refining of the alloys because impurities with a boiling temperature lower than the organic powder (e.g. water) should have condensed on the cap of the glass container. A similar refining procedure of the hygroscopic NPG was reported by Barrio et al. [1]. When the alloy was fully solidified, the glass container was crushed and the waxen alloy was ground and filled into a new storage container. From this container small amounts of the alloy were taken to fill the rectangle glass tubes.

For the filling, the rectangular glass tubes were laid on a hot plate such that one side was on the plate and the other side protruded freely. Small amounts of the alloy were deposited on the hot plate next to the open side of the tube. As soon as the alloy melted, the liquid was dragged into the tube by capillarity until it reached the colder side of the tube where it solidified. This procedure ensured that enough room for expansion due to melting (and heating) was left free. Next, the tube was slowly dragged off the hot plate allowing the material to solidify and then both ends were sealed. During the investigations in the Bridgman furnace, both ends of the tubes were outside of the Bridgman furnace and so kept around room temperature, so that the solid alloy further sealed the liquid part of the tube.

The Bridgman furnace consisted of a cold and a hot copper block with a distance of 4 mm. The hot zone block

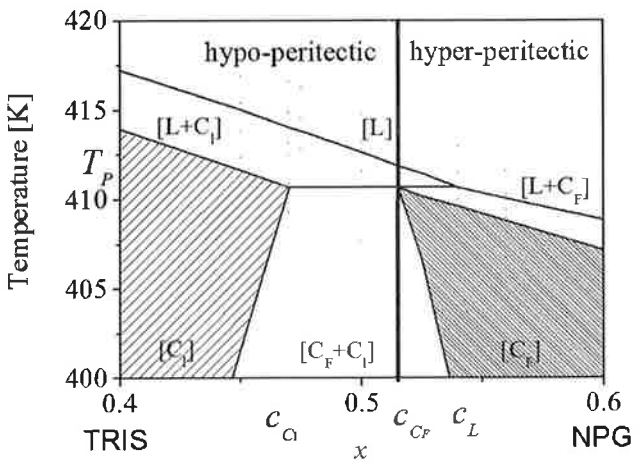

Fig. 1 : TRIS-NPG phase diagram as proposed by [1] and confirmed by [7]. The solidification phenomena reported in this work were observed from solidifying a hypo-peritectic alloy with c_0 = 0.5.

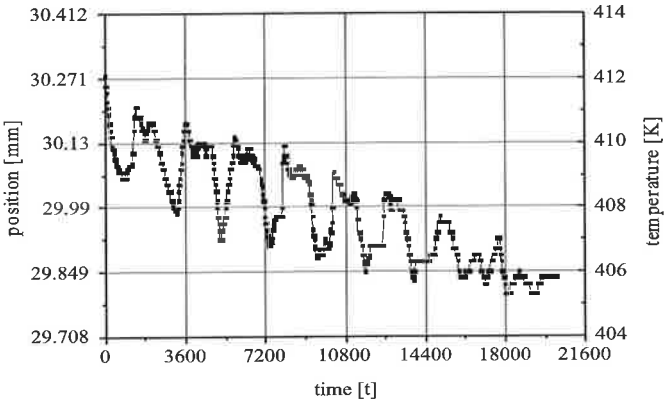

Fig. 2 : Oscillation of the interface/tip position and the corresponding interface/tip temperature as function of time for an hypo-peritectic TRIS-NPG alloy with c_0 = 0.5.

was heated to a temperature of 453 K using electric resistance heater, the cold zone temperature was controlled by a water circuit and set to a temperature of 353 K. The temperatures on both sides were measured with Pt 100 temperature sensors placed inside the copper blocks and regulated independently with an accuracy of ±0.1 K. The temperature gradients were measured with a 200 μm NiCr-Ni thermocouple within the filled large rectangle sample.). The measured gradient G = 14.2 K/mm was linear within the adiabatic/observation zone. The microscope was equipped with a CCD camera and self-developed software allowing the recording and storage of images and temperature data with a frame rate of up to 10 images per second. Furthermore, the software allowed the measurement of positions in the field of view.

Results and discussion

For an hypo-peritectic alloy with c_0 = 0.5 solidified with a pulling velocity V = 0.9 μm/s and a temperature gradient G = 14.2 K/mm, an *oscillatory growth* was observed. Figure 2 shows the oscillation of the interface/tip position and the corresponding interface/tip temperature as function of time. The gradual decay of the interface/tip temperature might be caused by the occurrence of macrosegregation amplified by convection and/or the decomposition of the organic alloys within the hot zone. A typical oscillation cycle reveals a period of ΔT = 2200 s which corresponds to a cycle length of Λ = 2 mm. In the following, an explanation of the oscillations is given based on a series of similar observations and further obvious arguments. However, it has to be mentioned that the two plastic phases which participate at a peritectic growth, namely [C$_I$] and [C$_F$], are optically undistinguishable. On the other hand, an interpretation of the oscillatory growth can be given if it is assumed that both phases grow simultaneously (but not necessarily at the same temperatures).

In Figs. 3-6, the evolution of growth morphology for the cycle from t = 7.050 s after start pulling to t = 9.360 s is shown. The cycle starts shortly before the minimum at t = 7.350 s occurs. The morphology evolution at the minimum is shown in Fig. 3 in more details. In Fig. 3a two cellular arrays can be seen, one slightly ahead of the other. In corresponding magnified pictures (not shown) it became clear that the two arrays grow at different depth in the sample. In order to understand the subsequent morphological transitions, let's assume that the leading array consists of [C$_I$]-cells and the following of [C$_F$]-cells. This assumption is only motivated by

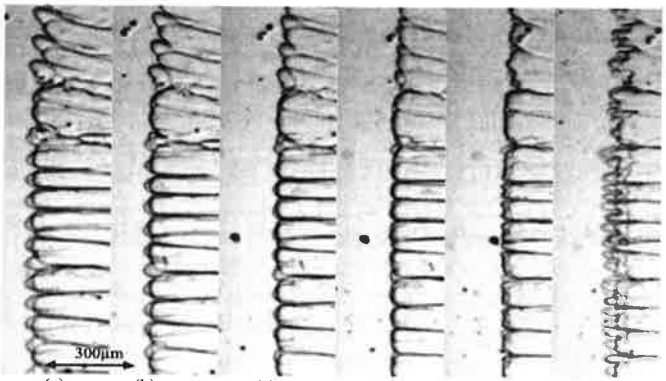

Fig. 3 : Growth of two cellular arrays close to the minimum interface/tip temperature. The front instability goes along with a minimum in interface/tip temperature. The pictures are taken t = 7.050 s after starting pulling with a time increment of Δt = 90 s.

the fact that for c_0 = 0.5 the [C_l]-phase has a higher liquidus temperature compare to the [C_F]-phase. Fig. 3a-d show that the advance of the [C_l]-cells gradually disappears until both cellular arrays grow with the same interface temperature. However, this "side-by-side" growth is obviously inherently unstable and leads to a sudden advance of smaller cells of both phases. The reason for this instability is not yet understood. Careful observation of morphological details makes it obvious that after the advance of the small cells of both phases the [C_l]-cells once more move ahead of the [C_F]-cells (see Fig. 4).

The leading fine [C_l]-cells further develop into dendrites, as can be seen in Fig. 5a. These isolated dendrites grow clearly ahead of the cellular front which might now consist mostly of [C_F]-cells. One might expect that the [C_l]-dendrites now gradually try to reach steady-state. However, what happens is something else. Suddenly all growing objects, [C_l]-dendrites and [C_F]-cells, shot forwards, as can be seen in Fig. 5b-d. This can be understood by considering the fact that a flat growth front which consists of deep cells (as shown in Fig. 2) does have a large solute layer similar to a planar front. With V = 0.9 µm/s and D = 3×10^{-10} m^2/s the boundary layer can be calculated to be δ =330 µm in thickness. After the sudden occurrence of the fine cellular growth, these cells have to grow right into the solute boundary layer. Due to the fact that the tip radius of the fine cells is much smaller than that of the former larger cells, the corresponding growth diffusion field is more or less localized around the tips. Therefore, the growth velocity can increase for both, the leading [C_l]-cells/dendrites as well as the following [C_F]-cells. This leads to a gradually forward motion of the front until the front reaches the end of the boundary layer. Here, the corresponding tips feel the initial melt composition and can therefore further accelerate until they reach a temperature close to the related steady-state tip temperature for the fast growth. This happens in Fig. 5d. However, now the tips have to adapt to the pulling speed and therefore the tip radii gets larger and larger (Fig. 5d-f). Note that the [C_l]- and [C_F]-tips do thicken at slightly different temperatures. The reason for that is that due to the higher liquidus temperature of [C_l], compared to [C_F], and due to an approximately similar tip undercooling, the tip temperature of [C_l] is higher than that of [C_F]. This argument confirms that the assumption of [C_l] being the leading phase is reasonable.

It is important to notice that as soon as the tips adapt to the pulling velocity, the maximum of the interface/tip temperature cycle is reached. With the following tip

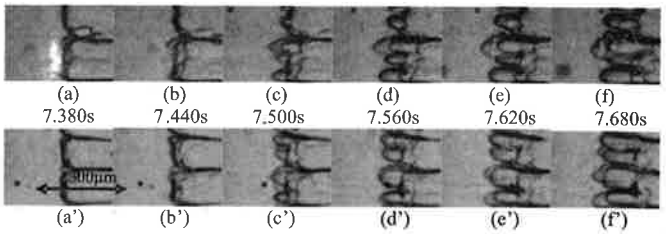

Fig. 4 : Two examples which show that after new finer cells of both phases occur, the fine [C_l]-cells are leading against the fine [C_F]-cells. In pictures (f) and (f') [C_l] is again the leading phase. The pictures are taken at t = 7.380 s after starting pulling with a time increment of Δt = 60 s.

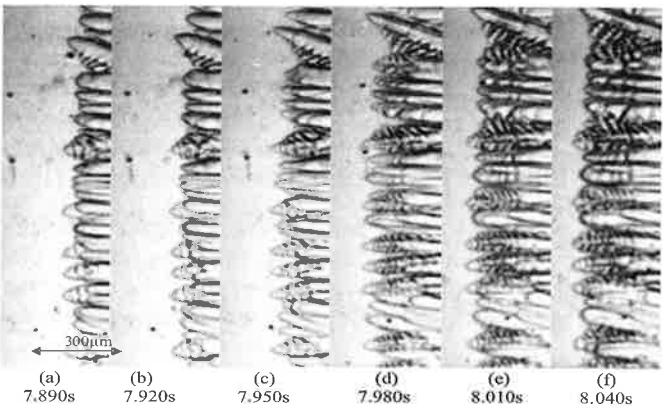

Fig. 5 : The leading [C_l]-dendrites as well as the following [C_F]-cells advance gradually until they reach the end of the solute boundary layer being formed previously. Then the tips accelerate strongly until the tip temperatures are close to the related steady-state tip temperature for the fast growth. Then the tip velocity adapts to the pulling speed and tip thickening occurs. The pictures are taken t = 7.890 s after starting pulling with a time increment of Δt = 30 s.

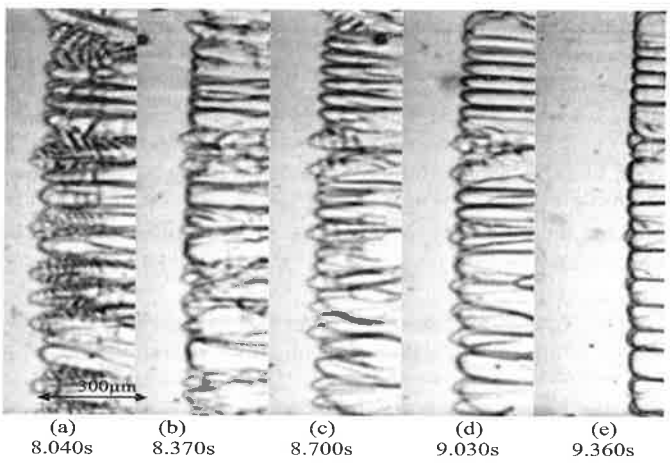

Fig. 6 : After reducing the growth velocity in order to adapt the pulling speed, tip thickening results in a transition from dendrite-like into cell-like growth. With that the interface/tip temperature decreases. Note that the [C_l]-cells/dendrites keep being ahead of the subsequently [C_F]-cells. The pictures are taken t = 8.040 s after starting pulling with a time increment of Δt = 330 s.

thickening (see Fig. 5e-f) a change from isolated-tip-growth to a diffusion-field-overlapping-growth occurs. In consequence the tip temperatures decrease again. The difference in tip temperatures between the [C_l]-cells and [C_F]-cells remains, while the interface/tip temperature further

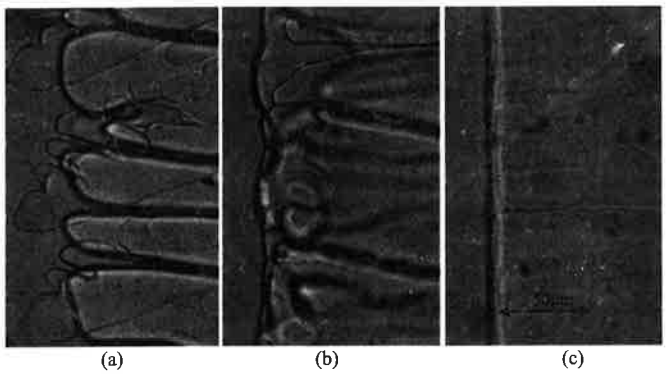

(a) (b) (c)

Fig. 7 : Development of coupled peritectic growth morphology by reducing the pulling velocity from 1.3 μm/s (a) down to 0.1 μm/s (c). The transition took around 3.7 hours. The pictures are taken with approximately 1.8 hours time interval. In the original video the coupled growth of the two solids is clearly visible. However, as static picture the contrast is quite low and thus the alternative occurrence of the different phases is hardly visible.

drops. Fig. 6 shows the evolution of the interface morphology from the maximum of the interface/tip temperature to its minimum. Note that Fig. 6e, taken at the end of the corresponding cycle, is similar to Fig. 3c, which represent the beginning of the cycle.

The oscillatory growth described here is different from the formation of an alternating sequence of α and β bands parallel to the solidification front (banded microstructures). Alternative bands form for growth velocities below the limit of constitutional undercooling (planar front growth), whereas here the growth velocity is definitely larger. In addition, we believe that in our case the [C_l]-phase is always the leading phase, and thus no change of the leading phase occur. Unfortunately, our in-situ observations do not allow to give confirmed information about the consequences of this oscillatory growth mode on the final microstructure. At least, the difference between coarse cellular and fine dendritic growths should be visible in a micrograph if high temperature coarsening is slowly.

Beside the oscillatory growth mode presented above, we have also directly observed the isothermal *coupled peritectic growth*. For this to happen, we have solidified the c_0 = 0.5 TRIS-NPG alloy with a relatively large velocity of V = 1.3 μm/s (above the limit of constitutional undercooling) and then deduced the pulling speed to V = 0.1 μm/s. The gradient was kept constant at G = 14.2 K/mm. Figure 7 shows the resulting change of the growth morphology.

The formation of the isothermal coupled peritectic growth started from the oscillatory growth described above. Fig. 7a shows [C_l]-dendrites ahead of [C_F]-cells similar to the situation shown in Fig. 5. On reducing the withdrawal speed the phases tend to form two planar solid/liquid interfaces, [C_l] in the background and [C_F] in the front. As the [C_l] and [C_F] interface morphologies get closer and closer to planarity they approach each other. By careful observation of corresponding video sequences it becomes obvious that [C_l]-phase start to form islands at the planar liquid/[C_F] interface (not shown here), which then form lamella which grow side-by-side with [C_F]-lamella. The typical wavelength of the isothermal couple peritectic growth, the lamella size, the exact solid/liquid interface form especially in the middle plane of the lamella and at the three junction point, all that is subject of ongoing studies. Note that we have also observed wavelike lamella with a typical wavelength larger than the lamella size.

Conclusions

In the present paper, we have presented in-situ observation of an oscillatory growth of a near-peritectic alloy which occurred for growth velocities above the limit of constitutional undercooling and in-situ observation of isothermal couple peritectic growth. The oscillatory growth turned out to be different from the formation of an alternating sequence of α and β bands parallel to the solidification front. The starting point for the present oscillations is a side-by-side growth of arrays of α- and β-cells. Both arrays of cells try to form a more or less planar growth front, until a sudden instability leads to the formation of fine cells of both types, which are now able to grow faster. The fine cells propagate until they reach the end of the solute boundary layer which was piled-up during "planar" cellular growth. After having grown beyond the boundary layer, the tips accelerate again until they reach a temperature close to the related steady-state tip temperature for the fast growth. Afterwards, the tips thicken again and thus the interface/tip temperature starts to drop. Close to a "planar" growth of the two cellular arrays the oscillation starts again. The described mechanism for an oscillatory growth had, to the authors' knowledge, never been observed before.

Acknowledgments

This work was funded by the European Space Agency ESA and the Austrian Space agency ASA through means of the ESA MAP project METCOMP.

References

1. Barrio M, Lopez D O, Tamarit J Ll, Negrier P and Haget Y, *J. Mater. Chem.*, **5** (1995) 431.
2. Witusiewicz V T, Sturz L, Hecht U and Rex S, *Acta Mater.* **52** (2004) 5519.
3. Sturz L, Witusiewicz V T, Hecht U and Rex S, *J. Crystal Growth* **270** (2004) 273.
4. Witusiewicz V T, Sturz L., Hecht U and Rex S, *Acta Mater.*, **53** (2005) 173.
5. Akamatsu S and Faivre G, *Phys. Rev. E*, **58** (1998) 3302.
6. Akamatsu S, Plapp M, Faivre G and Karma A, *Phys. Rev. E*, **66** (2002) 0305011.
7. Mogeritsch J, Grasser M and Ludwig A, *Scripta Metal.*, **60** (2009) 882.
8. Trivedi R, *Metall. Mat. Trans. A*, **26** (1995) 15.
9. Lograsso A, Fuh B C and Trivedi R, *Metall. Mat. Trans. A*, **36** (2005) 1287.
10. Hunzinger O, Vandyoussefi M and Kurz W, *Acta Mater.*, **46** (1998) 6325.
11. Dobler S, Lo T S, Plapp M, Karma A and Kurz W, *Acta Mater.*, **52** (2004) 2795.
12. Dobler S and Kurz W, *Z. Metallkd.*, **95** (2004) 592.
13. Dobler S, *PhD thesis*, EPFL, Lausanne, Switzerland (2001).
14. Kohler F, Germond L, Wagnière J and Rappaz M, *Acta Mater.*, **57** (2009) 56.
15. Kohler F, *PhD thesis*, EPFL, Lausanne, Switzerland (2008).
16. Kerr H W and W Kurz, *Int. Mater. Rev.*, **41** (1996) 129.
17. Lee J H and Verhoeven J D, *J. Cryst. Growth*, **144** (1993) 353.
18. Hunt J D and Chilton J P, *J. Inst. Met.*, **92** (1963-64) 21.
19. Mathiesen R H, Arnberg L, Mo F, Weitkamp T and Snigirev A, *Physical Review Letters*, **83** (1999) 5062
20. Nguyen-Thi H, Reinhart G, Mangelinck-Noel L, Jung H, Billia B, Schenk T, Gastaldi J, Hartwig, J and Baruchel J, *Metall. Mat. Trans. A*, **38** (2007) 1458
21. http://www.sigmaaldrich.com.
22. http://fscimage.fishersci.com (search for 126-30-7 and 77-86-1).
23. http://www.vitrocom.com.